Niclosamide ethanolamine improves blood glycemic control and reduces hepatic steatosis in mice

Hanlin Tao, Yong Zhang, Xiangang Zeng, Gerald I. Shulman, and Shengkan Jin

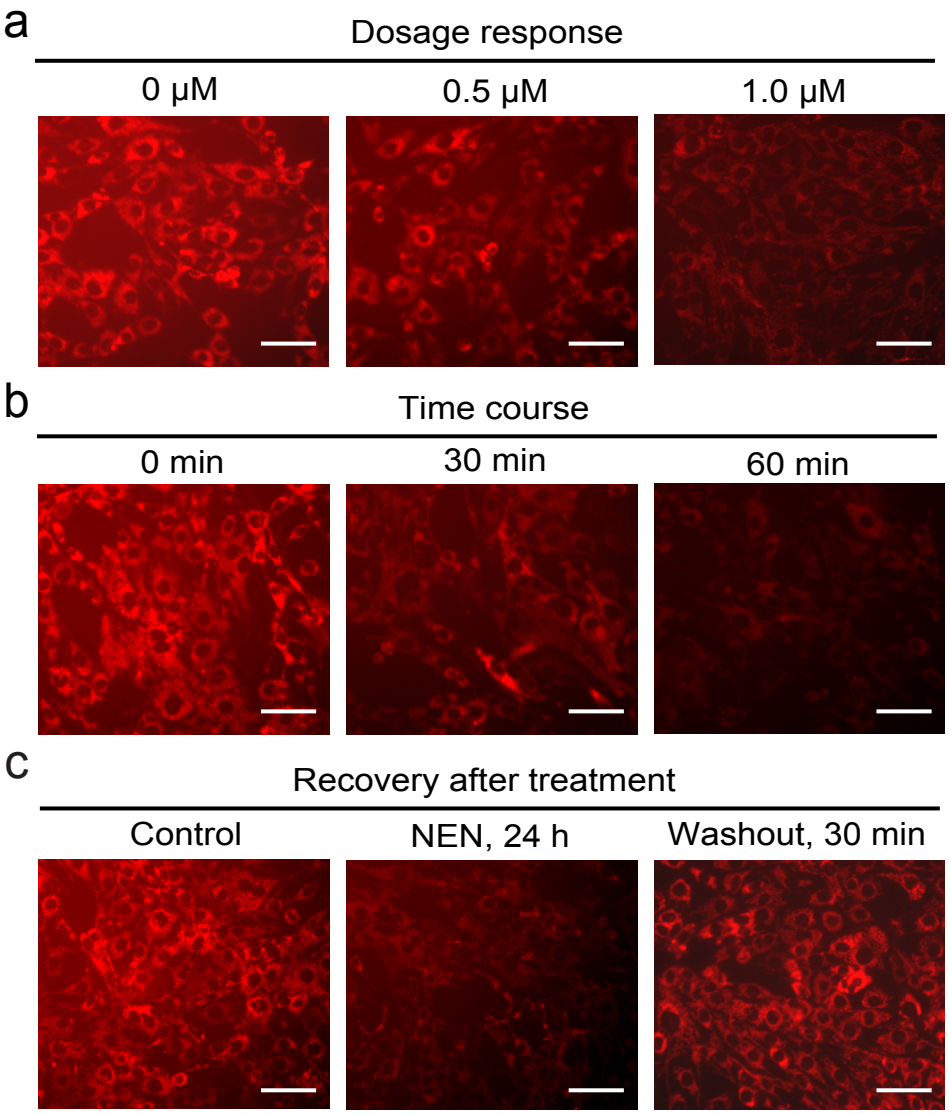

Supplementary Figure 1 NEN decreases mitochondrial membrane potential in live cells. TMRE staining of the NIH-3T3 cells (**a**) treated with NEN at indicated concentrations for 2 h, (**b**) treated with 1.0 μM NEN for indicated period of time, (**c**) treated with 1.0 μM NEN for 24 h followed by incubating in NEN free media for 30 min. TMRE was added to a final concentration at 100 nM for 10 min for mitochondrial membrane potential detection. Scale bars, 200 μm.

a

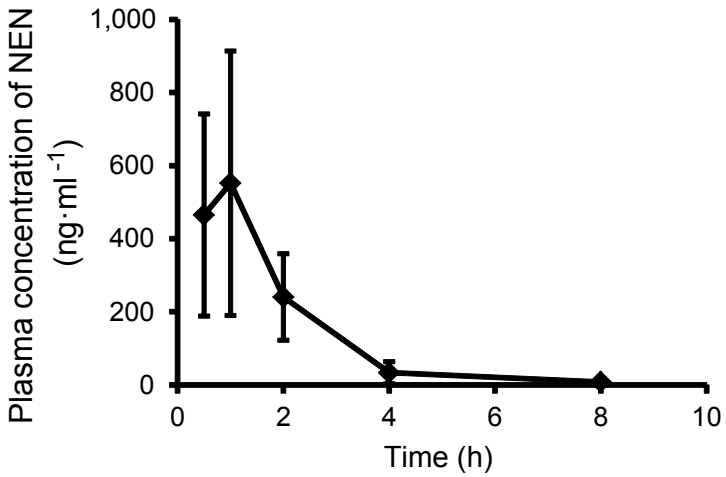

b

Pharmacokinetics of oral NEN

Dose (mg·kg^{-1})	$T_{1/2}$ (h)	Tmax (h)	Cmax (ng·ml^{-1})
40.0	1.25±0.36	0.58±0.38	644±292

c

Tissue distribution of oral NEN

Time points (h)	Liver (ng·g^{-1})	Muscle (ng·g^{-1})	Adipose (ng·g^{-1})	Brain (ng·g^{-1})	Heart (ng·g^{-1})	Lung (ng·g^{-1})	Spleen (ng·g^{-1})	Kidney (ng·g^{-1})
2	373.0±59	N.D.[a]	N.D.[a]	27.9±23	53.8±22	87.2±70	N.D.[a]	257.0±47
4	547.0±32	N.D.[a]	N.D.[a]	N.D.[a]	12.5±2	23.8±13	N.D.[a]	102.0±23
8	50.9±39	N.D.[a]	N.D.[a]	N.D.[a]	N.D.[a]	13.2±5	N.D.[a]	48.6±20

a: N.D., not detectable.

Supplementary Figure 2 Pharmacokinetic study of NEN in mice. (**a**) Plasma concentrations of NEN in male C57BL/6J mice followed by an oral administration of NEN at the dosage of 40 mg·kg^{-1} b.w. (**b**) Key pharmacokinetic parameters of NEN in mice. (**c**) Tissue distribution of NEN in mice under treatment as defined in **a**, at indicated time points. Data are expressed as means ± s.d. and $n = 3$ for all groups.

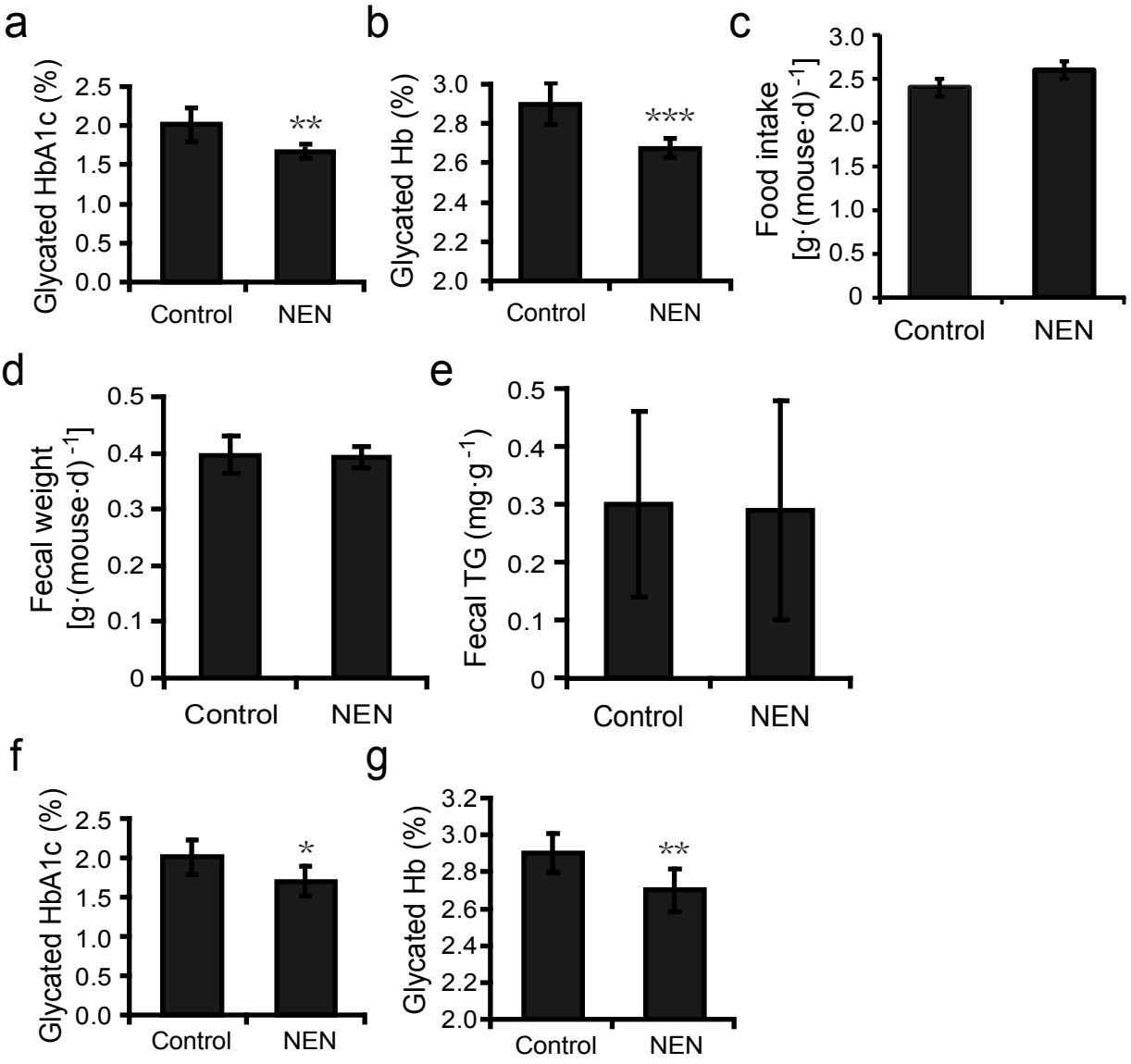

Supplementary Figure 3 Effect of NEN on HFD treated mice. (**a**) Glycated hemoglobin A1c (HbA1c) levels, and (**b**) total glycated hemoglobin (Hb) levels of male C57BL/6J mice fed with HFD (control) or HFD containing 1,500 ppm NEN (NEN) for 16 wk. (**c**) Daily food intake, (**d**) daily fecal productions, and (**e**) fecal triglyceride contents, of male C57BL/6J mice either fed with HFD (control) or HFD containing 1,500 ppm NEN (NEN). (**f**) Glycated hemoglobin A1c (HbA1c) levels, and (**g**) total glycated hemoglobin (Hb) levels of male C57BL/6J mice that were first fed with HFD for 16 wk, and then randomized into two groups either fed with HFD (control), or same HFD containing 1,500 ppm of NEN (NEN) for 4 additional wk. Data are expressed as means ± s.d. and $n = 7$ for all groups. Student t-test, $*P < 0.05$; $**P < 0.01$; $***P < 0.001$.

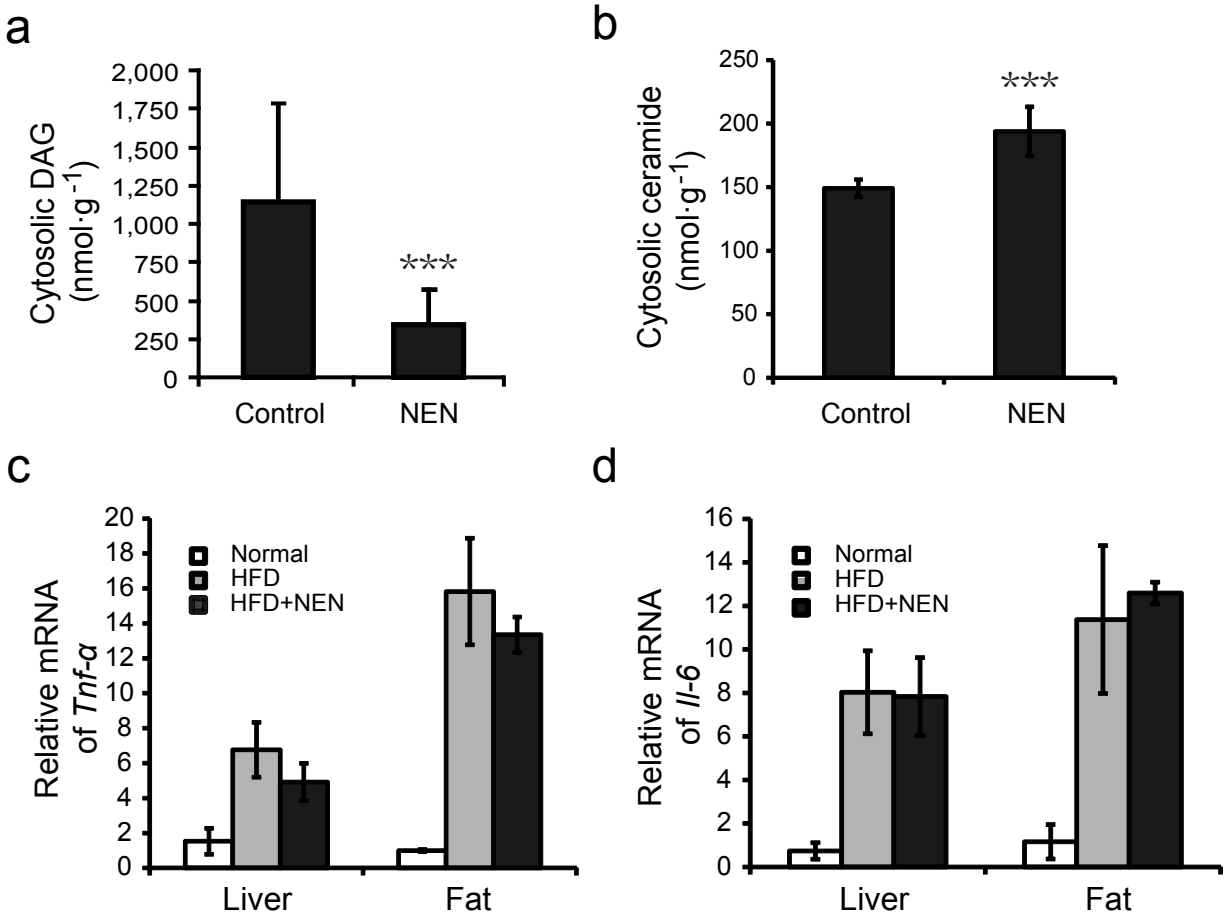

Supplementary Figure 4 Analyses of DAG, ceramide, *Tnf-α* and *Il-6*. (**a**) Cytosolic DAG concentrations, and (**b**) cytosolic ceramide concentrations in liver samples from male C57BL/6J mice fed with either HFD (control) or HFD containing 1,500 ppm NEN (NEN) for 8 wk, $n = 8$. Both the membrane associated and cytosolic DAG and ceramide concentrations of liver tissues were determined and normalized against tissue mass. Only the cytosolic concentrations are shown. (**c**) Relative mRNA levels of *Tnf-α*, and (**d**) *Il-6* in liver and white adipose tissues, as indicated, from mice as defined in **a**, $n = 3$. The mRNA levels of the indicated genes were analyzed by quantitative real-time PCR, normalized against the *Gapdh* expression levels. Data are expressed as means ± s.d., Student t-test, ***$P < 0.001$.

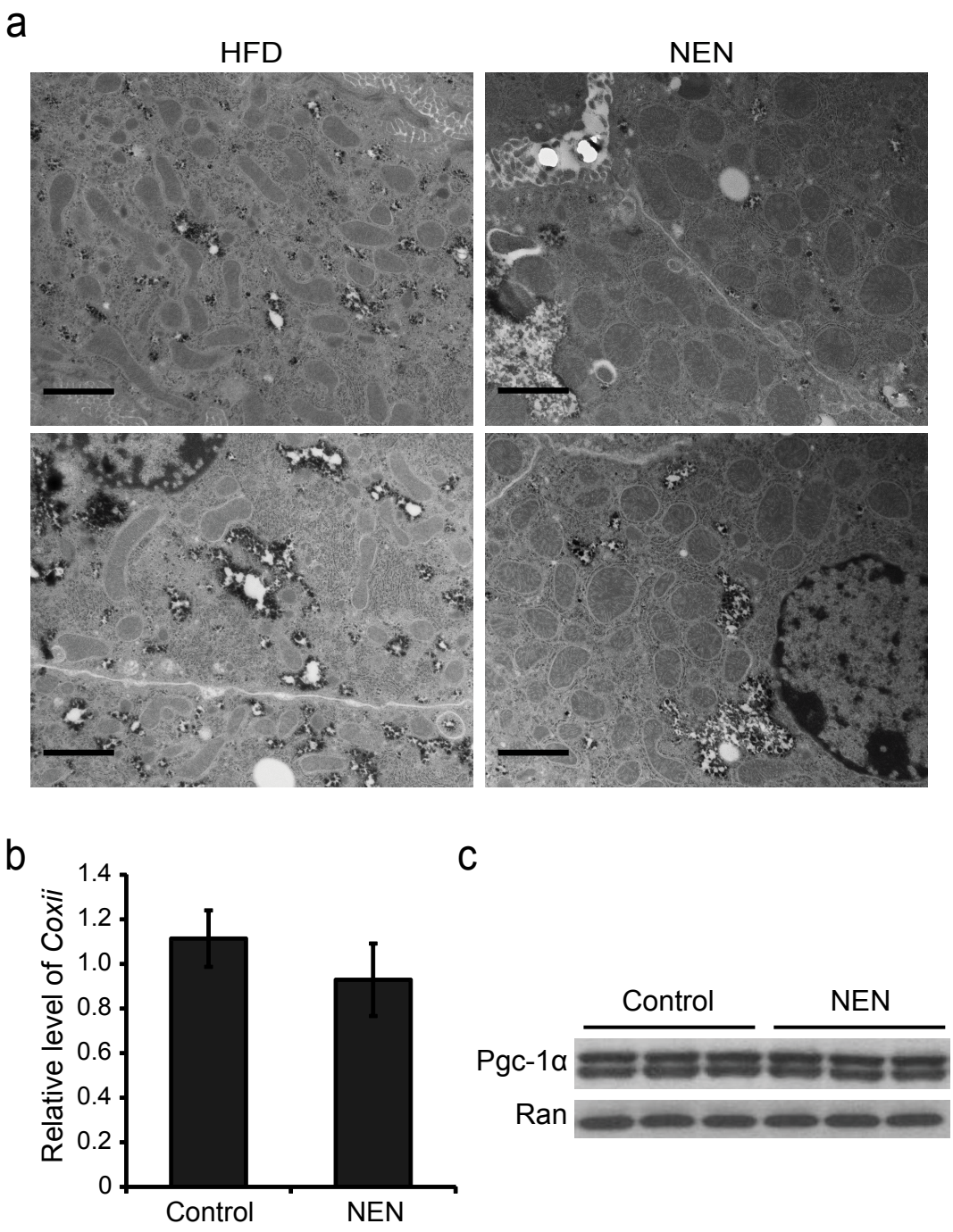

Supplementary Figure 5 Effect of oral NEN on mitochondrial morphology, mitochondrial content, and the expression of Pgc-1α. (**a**) Representative electronic microscopy images of liver tissues from male C57BL/6J mice fed with either HFD (control) or HFD containing 1,500 ppm NEN (NEN) for 16 wk. Scale bars, 2 μm. (**b**) Quantitative real-time PCR showing relative abundance of mitochondrial gene *Coxii*, from liver tissues of mice as defined in **a**. Data are expressed as means ± s.d., $n = 3$. (**c**) Immunoblotting analyses showing the protein levels of Pgc-1α from mice as defined in **a**.

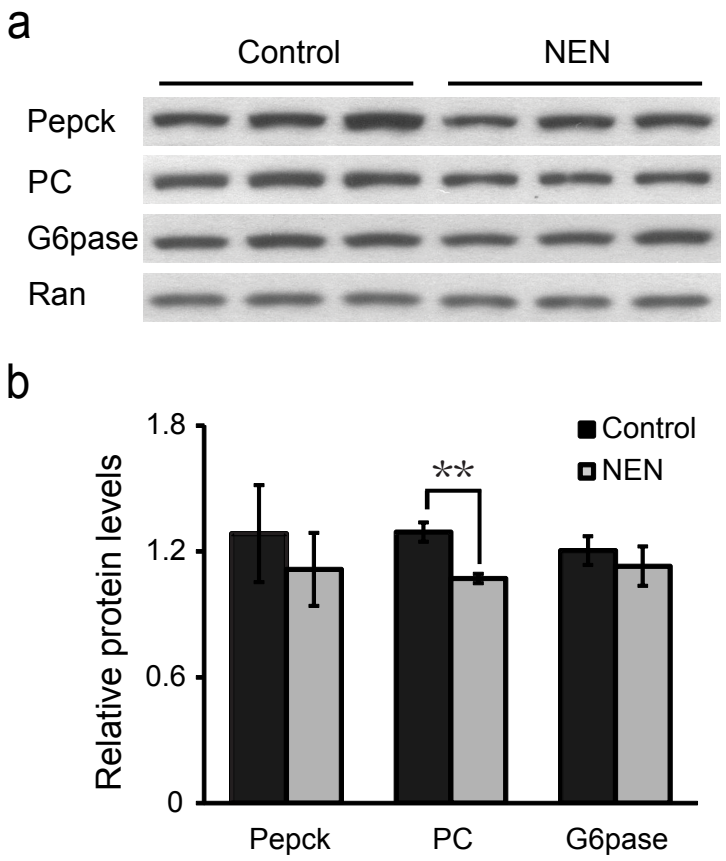

Supplementary Figure 6 Effect of oral NEN on the expression of key enzymes in hepatic gluconeogenesis. (**a**) Immunoblotting analyses of liver samples from male C57BL/6J mice fed with either HFD alone (Control) or HFD containing 1,500 ppm NEN (NEN) for 8 wk. Pepck, phosphoenolpyruvate carboxykinase; PC, pyruvate carboxylase; G6pase, Glucose-6-phosphatase. $n = 3$. (**b**) Quantification of **a**. Data are expressed as means ± s.d., Student t-test, $^{**}P < 0.01$.

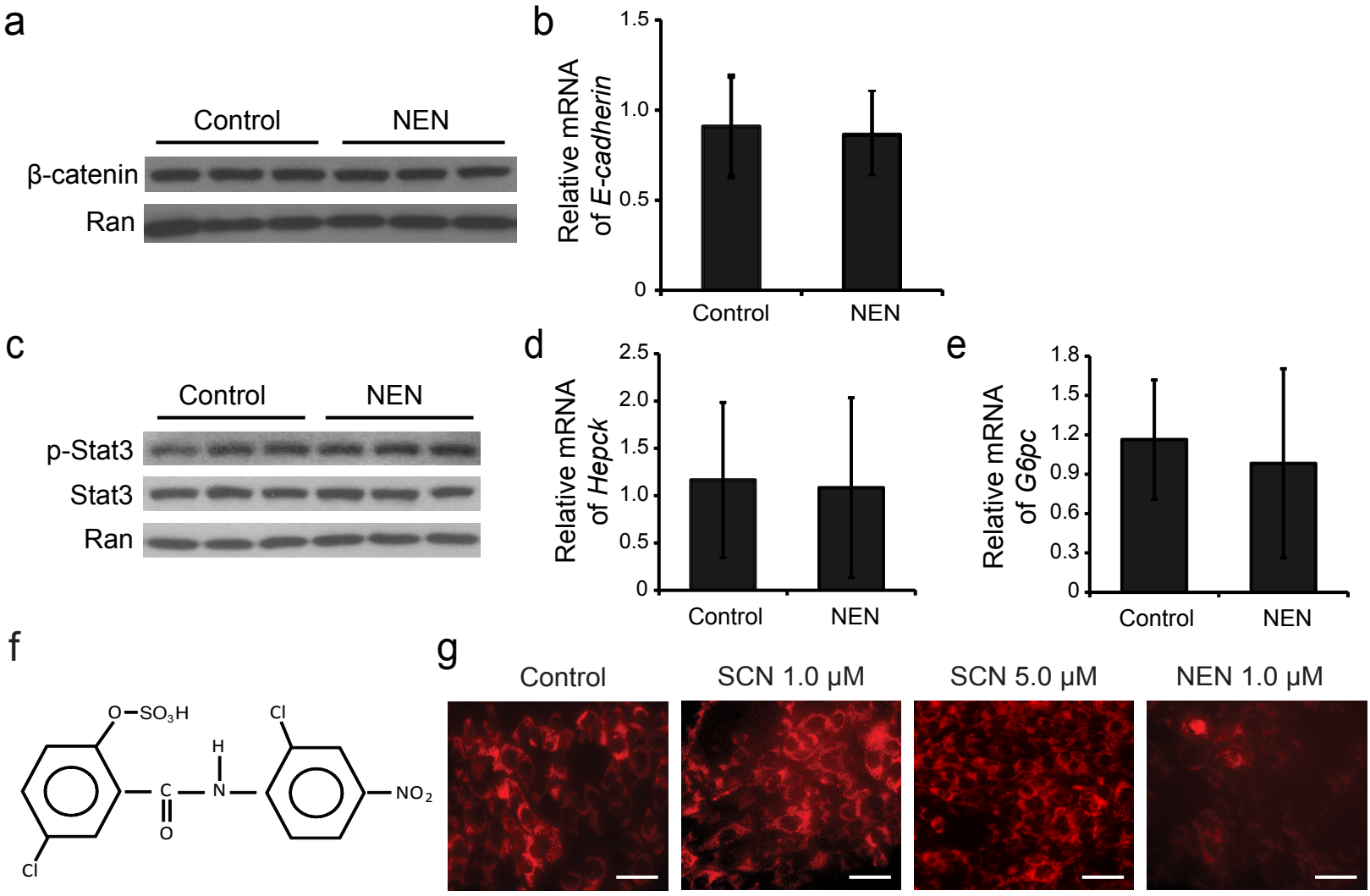

Supplementary Figure 7 Effect of NEN on Wnt and Stat3 pathways *in vivo* and characterization of sulfonated niclosamide at 2-hydroxyl position. (**a**) Immunoblotting analyses of β-catenin, and (**b**) quantitative real-time PCR analyses of relative mRNA abundance of *E-cadherin* in liver samples from male C57BL/6J mice fed either with HFD alone (Control) or HFD containing 1,500 ppm NEN (NEN) for 8 wk. (**c**) Immunoblotting analyses of total Stat3 (Stat3) and phosphorylated Stat3 (p-Stat3), and (**d**) and (**e**) Quantitative real-time PCR analyses of relative mRNA abundance of *Hepck* and *G6pc,* as indicated, in liver samples from mice as defined in **a** and **b**. Data are expressed as means ± s.d., $n = 3$ for all groups. (**f**) Chemical structure of the sulfonate- conjugated niclosamide (SCN) at 2- hydroxyl position. (**g**) TMRE staining of the NIH-3T3 cells treated with SCN or NEN at indicated concentrations for 2 hours. TMRE was added to a final concentration at 100 nM for 10 min for mitochondrial membrane potential detection. Scale bars, 200 μm.

Supplementary Table 1. Body weight gain and fat mass change in HFD-fed mice

Treatment	Initial			16 wks		
	Body weight (g)	Fat mass (g)	Lean mass (g)	Body weight (g)	Fat mass (g)	Lean mass (g)
Control (*n*=11)	22.6±0.3	1.5±0.1	20.9±0.3	31.0±1.0	9.7±0.9	25.2±0.6
NEN (*n*=11)	21.5±0.5	1.4±0.1	19.8±0.5	26.0±1.0	5.8±0.5	23.1±0.6
p-value[a]	N.S. [b]	N.S. [b]	N.S. [b]	<0.001	<0.001	<0.05

Data are expressed as means ± s.d. **a:** Student t-test; **b:** N.S., No statistical significance.